Structure-dependent surface conductance at the initial stages in metal epitaxy on Si(111) surfaces

Shuji Hasegawa

Department of Physics, Faculty of Science, University of Tokyo, Hongo, Bunkyo-ku, Tokyo 113 (Japan),
and PRESTO, Research Development Corporation of Japan (JRDC) (Japan)

Shozo Ino

Department of Physics, Faculty of Science, University of Tokyo, Hongo, Bunkyo-ku, Tokyo 113 (Japan)

Abstract

Combination of reflection high energy electron diffraction and *in situ* measurements of surface conductance and Hall effect enables one to correlate atomic structures of surfaces and their macroscopic electrical properties. For initial deposition of Au and Cs onto clean Si(111)-7 × 7 and Au-induced superstructure (5 × 2, 6 × 6, $\sqrt{3} \times \sqrt{3}$) surfaces, the differences between them in terms of Fermi level pinning and band bending were revealed. Inversion layers were created at the Au-covered surfaces and changed into depletion layers on metal adsorption onto them, resulting in steep decrease in surface conductance, while the clean surface was much less sensitive in terms of band bending change on metal adsorption because of Fermi level pinning. The band bending of each surface is also supported by photoemission data.

The relation between the structural and electric properties of metal-covered semiconductor surfaces or interfaces has been extensively studied with many complementary experimental methods, especially from the point of view of Schottky barrier formation (see, for example, ref. 1). Several experiments with $NiSi_2$/Si [2], metal/GaAs [3], and Pb/Si [4–6], have demonstrated the dominant role of the intrinsic interfacial electronic structures over macroscopic bulk parameters in determination of the Schottky barrier height (SBH). The Fermi level pinning and band bending at interfaces, governing the SBH, inevitably depend on the atomic bonding and local electronic structures at the interface.

In our previous papers [7, 8], we found that, at the initial stages of Ag and Au depositions onto Si(111) surfaces at room temperature (RT), the conductance parallel to the surface crucially depended on the surface structures and epitaxial growth styles of the metal films. In the case of Ag deposition onto Si(111)-$\sqrt{3} \times \sqrt{3}$-Ag surfaces, the conductance exhibited a steep increase with low Ag coverage, less than 1/10 monolayer (ML), while it scarcely changed for Ag deposition onto a clean 7 × 7 substrate. Au depositions onto Si(111)-5 × 2, $\sqrt{3} \times \sqrt{3}$, and 6 × 6-Au surfaces gave rise to abrupt decreases in conductance at the beginning of deposition. For Au adsorption onto a clean 7 × 7 surface, on the contrary, a much smaller change at the same coverage region resulted.

Following the established understanding of the conductance changes of semiconductor surfaces on foreign material adsorption [9], our observed characteristic changes in conductance were attributed to changes in surface space charge layers in the Si substrate, governed by the Fermi level pinning and band bending. UV photoelectron spectroscopy (UPS) for a clean Si(111)-7 × 7 surface reveals a "metallic edge", sufficient density of surface states for the Fermi level pinning (for a review see ref. 10), resulting in an insensitive response in the surface conductance on metal adsorption. An Si(111)-$\sqrt{3} \times \sqrt{3}$-Ag surface, on the contrary, has no intensity at the Fermi level in UPS spectra, *i.e.* it is a "semiconducting surface" [11, 12], which allows an easy shift of the Fermi level and change in band bending on adsorption of a small amount of metal atoms, leading to a steep change in surface excess carrier concentration. The same mechanism is expected also for the Au-induced superstructure surfaces, because of the weak "pinning force", *i.e.* negligible density of states for Fermi level pinning.

In the present paper, in order to confirm speculation on the mechanism of the conductance changes mentioned above, the Hall coefficient was simultaneously measured during metal deposition with reflection high energy electron diffraction (RHEED) observations in an ultrahigh vacuum environment. The carrier concentration was found to change in a consistent way expected from the band bending picture. The results are also discussed with angle-resolved UPS experiments [13].

An n-type Si(111) wafer was used and the surface preparation procedures were as previously described [7,
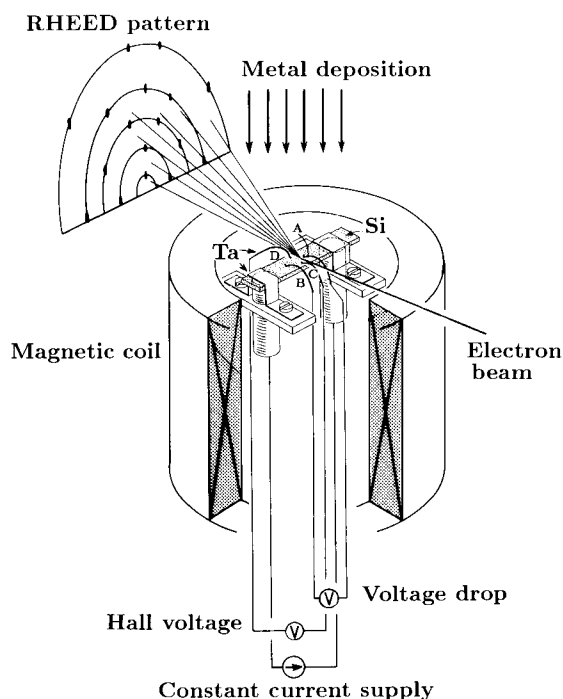
RHEED pattern

Fig. 1. The sample holder, drawn upside down.

Fig. 2. Resistance changes during RT Au depositions onto (a) clean Si(111)-7 × 7 and (b) Si(111)-5 × 2-Au, and (c) RT Cs deposition onto Si(111)-5 × 2-Au surfaces. The measuring current $I = 10\,\mu A$. Changes in RHEED patterns are indicated.

8]. As shown in Fig. 1, the conductance of the central portion of the wafer, under isothermal conditions at RT, was measured as a voltage drop between a pair of Ta wire contacts (0.4 mm in diameter), A and B, kept in contact by elasticity, with a constant current of 10 or 200 μA supplied through the Ta rod electrodes. The Hall voltage was simultaneously measured through another pair of Ta wire contacts, C and D. The magnetic field of ±230 G, which was nearly perpendicular to the surface, was applied with a coil composed of a ceramic-coated Al–Cu wire. The surface structural changes could be analysed with RHEED at 15 kV acceleration when the magnetic field was turned off. Au was evaporated with constant rates from Al_2O_3-coated W baskets which were placed about 50 cm away from the Si substrate. Cs was deposited with an SAES dispenser (from SAES Getters), mounted about 25 cm away. Since the primary electron beam current of about 1 μA in RHEED disturbed the voltages between the Ta wire contacts, the beam was always turned off during the measurement, except for the intermittent observations of the RHEED patterns in the course of metal deposition.

Figure 2 shows the changes in resistance between the Ta wire contacts A and B in Fig. 1 during Au deposition (rate, 0.21 ML min⁻¹) at RT onto a clean 7 × 7 surface (Fig. 2(a)) and onto a 5 × 2-Au surface (Fig. 2(b)), and Cs deposition onto a 5 × 2-Au surface (Fig. 2(c)). A remarkable feature in Fig. 2(b), in contrast to Fig. 2(a), is an abrupt large increase in resistance just after the evaporator shutter was opened. Similar
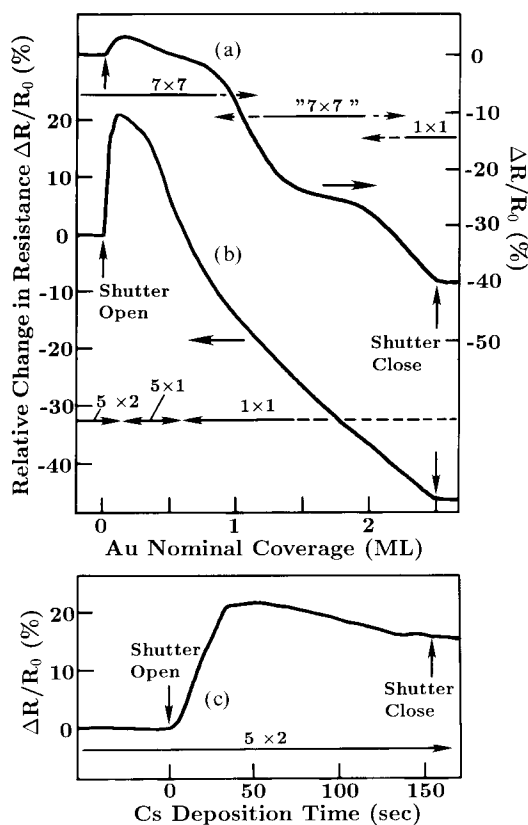
changes were observed for other Au-induced super-structure surfaces ($\sqrt{3} \times \sqrt{3}$ and 6 × 6) [8]. Cs deposition (Fig. 2(c)) onto the 5 × 2-Au surface produced a change similar to that in Fig. 2(b); a large increase in resistance at the beginning. These results suggest that adatoms of Cs and Au on the 5 × 2-Au surface act electrically in a similar way.

Figure 3 shows changes in resistance (between the contacts A and B) and the Hall voltage (between the contacts C and D) during RT Au deposition onto the Si(111)-6 × 6-Au surface and during its interruption. During the deposition periods, the resistance changed in a similar way to that of the 5 × 2-Au surface (Fig. 2(b)); a large increase at the beginning followed by a subsequent decrease. Because the contact pair C and D was not perfectly perpendicular to the current direction, the resistance change was also picked up with the pair. The Hall voltage was measured during the interruption periods of deposition by applying a 230 G magnetic field and turning over the field direction. The Hall voltage increased from 76.1 μV (corresponding to a Hall coefficient $R_H = -3.3 \times 10^4\,cm^3\,C^{-1}$) to 95.1 μV ($R_H = -4.2 \times 10^4\,cm^3\,C^{-1}$), accompanying the initial
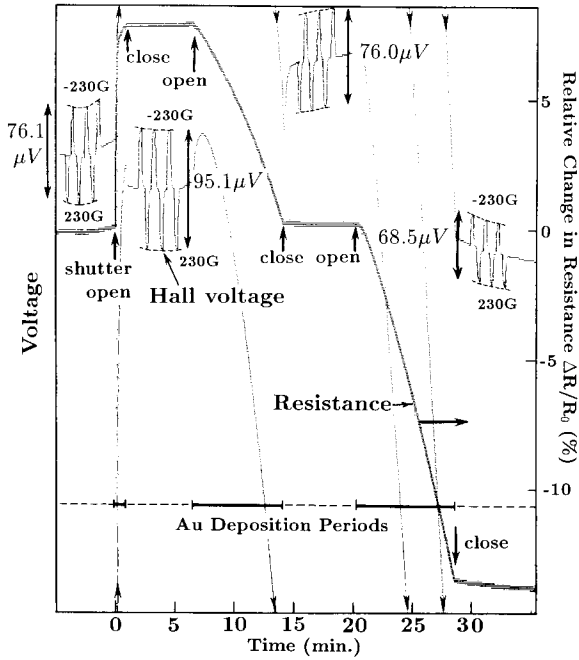
Fig. 3. Changes in resistance and Hall voltage during RT Au deposition onto an Si(111)-6 × 6-Au surface ($I = 200$ μA).

Fig. 4. Normal emission UPS spectra taken from an Si(111)-7 × 7 clean surface and Si(111) surfaces with Au-induced superstructures (reproduced from ref. 13).

increase in resistance immediately after the Au deposition started: this indicates a decrease in the carrier concentration. Followed by the subsequent decrease in resistance, the Hall voltage also dropped. Although the measured Hall voltage includes the contribution from the carriers in the inner bulk region, its change was actually caused by Au atom adsorption.

The observed changes in resistance and Hall voltage are understood with the aid of the photoemission data of Fig. 4 [13]. This figure shows normal emission UPS spectra from Si(111)-7 × 7 clean, -5 × 2-Au, -α-$\sqrt{3} \times \sqrt{3}$-Au, -β-$\sqrt{3} \times \sqrt{3}$-Au and -6 × 6-Au surfaces which were excited with He I radiation (21.2 eV). The well-known surface states S_1 and S_2 of the clean 7 × 7 surface are indicated [10]. At normal emission, a prominent peak B 1.9 eV below the Fermi level E_F is known to correspond to a bulk feature, not to another surface state S_3 [10, 14]. For the surfaces with Au-induced superstructures, this bulk peak survives as small peaks indicated by arrowheads, the positions of which are observed to shift toward E_F compared with the position at the 7 × 7 surface; shifts of 0.4–0.6 eV are seen. This means that upward band bendings take place at the surfaces. The upward band bendings for Si(111) surfaces with Au-induced superstructures were also observed in core level shifts in X-ray photoelectron spectra [15]. Because the Fermi level of the clean 7 × 7 surface is pinned at the S_1 surface state, 0.63 ± 0.05 eV above the valence band maximum (VBM) edge [16, 17], the Fermi level at the surfaces with the Au-induced superstruc-tures is then concluded to be located around
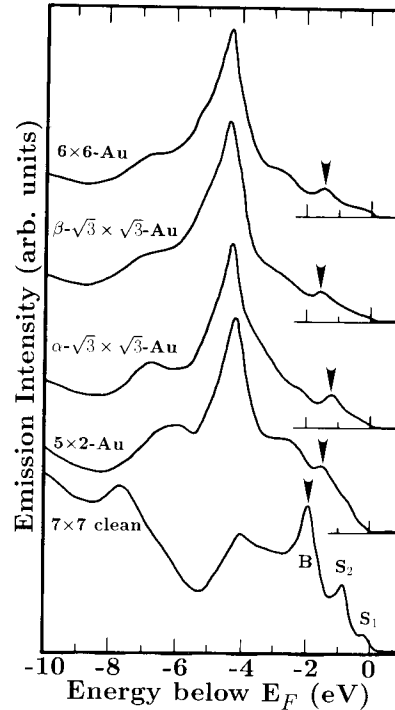
the VBM, resulting in a p-type inversion layer on an n-type Si substrate (Fig. 5(a)).

It is well known that Cs atoms adsorbed on a semi-conductor surface donate electrons into the semiconductor [18]. Therefore it is expected that Au as well as Cs (both are group I elements) adsorbed on the Au-induced superstructure surfaces will make donor-like surface states near the conduction band minimum edge. This makes the bands bend downward, and converts the p-type inversion layer into a depletion layer, from Fig. 5(a) to Fig. 5(b), resulting in a decrease in the carrier concentration near the surface region (Fig. 5(e)). Since a very small number of adatoms is enough to cause such variation, the resistance increased steeply just after the deposition started. This mechanism is consistent with the observed change in the Hall voltage. These changes are in distinct contrast to the insensitivity of the 7 × 7 surface on metal adsorption, in which a strong E_F pinning by a surface state with a large density of states is at work (Fig. 5(d)). The subsequent decreases in resistance after the maxima in Figs. 2(b) and 3 are reached are not clearly understood at present; they may be caused by further downward band bending to create an accumulation layer, from Fig. 5(b) to Fig. 5(c), or upward bending returning to an inversion layer, to Fig. 5(a) from Fig. 5(b), or by percolation conduction through a metallic surface layer.
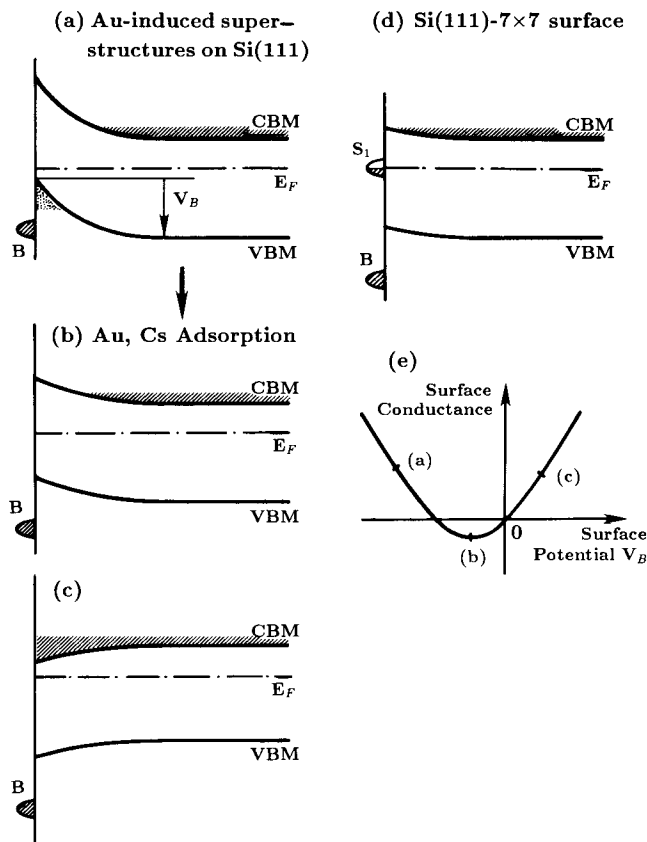
(a) Au-induced super-structures on Si(111)

(b) Au, Cs Adsorption

(c)

(d) Si(111)-7×7 surface

(e)

Fig. 5. (a)–(d) Schematic band diagrams at each surface (CBM, conduction band minimum; VBM, valence band maximum; E_F, Fermi level; B, bulk state indicated by arrowheads in Fig. 4): (a) Au-induced superstructures on Si(111); (b) Au or Cs adsorption onto the surface of (a); (c) Possible band bending by further Au adsorption onto the surface of (b); (d) Si(111)-7 × 7 surface. (e) Surface conductance vs. surface potential V_B.

In this way, the dependence of the surface conductance changes for initial metal adsorption on the well-defined substrate–surface structures reveals a direct correlation between microscopic atomic or electronic structures and the macroscopic electrical properties of surfaces. These investigations may not only be useful for understanding the Schottky barrier formation, but also lead to the possibility of novel microelectronic devices by modulating surface–interface structures.

References

1 G. LeLay, J. Derrien and C. A. Sébenne (eds.), Proc. Int. Conf. on the Formation of Semiconductor Interfaces (ICFSI), in Surf. Sci., 168 (1987). A. Hiraki, A. Kawazu and I. Ohdomari (eds.), ICFSI-2 in Appl. Surf. Sci., 41–42 (1989).
2 R. T. Tung, Phys. Rev. Lett., 52 (1984) 461.
3 S. Chang, L. J. Brillson, Y. J. Kime, D. S. Rioux, P. D. Kirchner, G. D. Petit and J. M. Woodall, Phys. Rev. Lett., 64 (1990) 2551.
4 G. LeLay, K. Hricovini and J. E. Bonnet, Appl. Surf. Sci., 41–42 (1989) 25.
5 D. R. Heslinga, H. H. Weitering, D. P. van der Werf, T. M. Klapwijk and T. Hibma, Phys. Rev. Lett., 64 (1990) 1589.
6 H. H. Weitering, A. R. H. F. Ettema and T. Hibma, Phys. Rev. B, 45 (1992) 9126.
7 S. Hasegawa and S. Ino, Phys. Rev. Lett., 68 (1992) 1192.
8 S. Hasegawa and S. Ino, in K. Terakura (ed.) Proc. 3rd Int. Symp. on Dynamical Processes at Solid Surfaces, Tokyo, 1992 in Surf. Sci., 283 (1993) 438.
9 A. Many, Y. Goldstein and N. B. Grover, Semiconductor Surfaces, North-Holland, Amsterdam, 1965. D. R. Frankl, Electrical Properties of Semiconductor Surfaces, Pergamon, Oxford, 1967.
10 G. V. Hansson and R. I. G. Uhrberg, Surf. Sci. Rep., 9 (1988) 197.
11 T. Yokotsuka, S. Kono, S. Suzuki and T. Sagawa, Surf. Sci., 127 (1983) 35.
12 J. M. Nicholls, F. Salvan and B. Reihl, Phys. Rev. B, 34 (1986) 2945.
13 Y. Tezuka, Master Thesis, University of Tokyo, 1987. H. Daimon, Y. Tezuka and S. Ino, to be published.
14 R. I. G. Uhrberg, G. V. Hansson, U. O. Karlsson, J. M. Nicholls, P. E. S. Persson, S. A. Flodstorm, R. Engelhardt and E. E. Koch, Phys. Rev. B, 31 (1985) 3795.
15 H. Daimon, personal communication, 1992.
16 F. J. Himpsel, G. Hollinger and R. A. Pollack, Phys. Rev. B, 28 (1983) 7014.
17 R. J. Hamers, R. M. Tromp and J. E. Demuth, Phys. Rev. Lett., 56 (1986) 1972.
18 G. Allen and G. W. Gobell, Phys. Rev., 144 (1966) 558.